Observations and Study of Byurakan-IRAS Galaxies: Summary

G. A. Mikayelyan*, A. M. Mickaelian, H. V. Abrahamyan, G. M. Paronyan, and M. V. Gyulzadyan

NAS RA V. Ambartsumian Byurakan Astrophysical Observatory, Armenia

Abstract

The paper is a summary and general analysis of optical spectroscopic data on 257 Byurakan-IRAS Galaxies (BIG objects) obtained with the BAO 2.6-m, SAO 6-m, OHP 1.93-m telescopes and taken from SDSS spectroscopic database. 149 star-formation regions galaxies, 42 galaxies with active nuclei, and 28 galaxies with a composite spectrum were identified. The spectra of 21 galaxies show signs of emission, but without the possibility of more precise determination of their activity type, 13 galaxies appear to have star formation rates that do not exceed normal, and 3 are absorption galaxies.

Keywords: *galaxies: spectra: active galactic nuclei: starburst galaxies*

1. Introduction

The InfraRed Astronomical Satellite (IRAS) was the first space-based observatory that performed a survey of the entire sky at infrared (IR) wavelengths. It mapped 96% of the sky in four bands: 12, 25, 60, and 100 μm. IRAS point sources are published in two large catalogues, IRAS Point Source Catalog (PSC; IRAS 1988) and IRAS Faint Source Catalog (Moshir et al., 1990). Though FSC contains fainter sources and is deeper, however, it misses the Milky Way area b $< |10°|$. In 2015, Abrahamyan et al. (2015) cross-correlated these two catalogues and the Combined Catalogue of IRAS point sources was published containing 345,163 sources. However, many of these sources are still left without any identification, that is, their physical nature remains unclear. Thus, the question of identifying these objects in the visible and obtaining optical spectra for classifying them has arisen. This may lead to a revision of previous ideas regarding the relative distribution of various types of galaxies. About 75,000 of them are believed to be starburst (SB) galaxies, still undergoing their star-formation phase. IRAS sources have increased our understanding of objects in Our Galaxy (stars and nebulae), especially star formation processes in galaxies, activity of galactic nuclei, and galaxy interactions. In particular, there is a special interest in the discovery of galaxies with high IR luminosity: LIRG (Luminous InfraRed Galaxies), ULIRG (Ultra-Luminous InfraRed Galaxies), and HLIRG (Hyper-Luminous InfraRed Galaxies) (Sanders and Mirabel, 1996). Latest IR surveys have shown that ULIRGs are vastly more numerous at high redshifts. Understanding the physics and evolution of ULIRGs, the contribution of high redshift ULIRGs to the cosmic IR background and the global history of star formation, and the role of ULIRGs as diagnostics of the formation of massive galaxies and large-scale structures are important questions still to be clarified. Though a number of recent IR (especially near-IR and mid-IR) surveys appeared: 2MASS (Cutri et al., 2003, Skrutskie et al., 2006); AllWISE (Cutri et al., 2013); AKARI (Ishihara et al., 2010, Yamamura et al., 2010), IRAS catalogues are still useful for studies at far-IR (FIR) wavelengths (60 and 100 μm), i.e., for extragalactic studies, and IRAS galaxies provide homogeneous samples of IR-selected AGN and SB.

There have been a number of studies on identifications of IRAS galaxies since the release of IRAS catalogs: IRAS Revised Bright Galaxy Sample (Sanders et al., 2003); Far-InfraRed (FIR) sources

*gormick@mail.ru, Corresponding author

DOI: 10.52526/25792776-2019.66.1-31

(Bertin et al., 1997); IRAS galaxies towards the Boötes void (Strauss and Huchra, 1988); IRAS point sources in the area of Fornax, Hydra I and Coma clusters (Wang et al., 1991); IRAS 1.2 μm survey (Fisher et al., 1995); IRAS galaxies in Virgo cluster area (Yuan et al., 1996); and some others.

About half of all IRAS sources are still not identified and there is a need for optical identifications. Since 1995, a project of optical identifications has been carried out in the Byurakan Astrophysical Observatory (Mickaelian, 1995), in order to detect new galaxies with bursts of star formation in their central regions (SB, or Starburst galaxies) (Weedman et al., 1981), galaxies with active nuclei (AGN, active galactic nuclei) (Ambartsumian, 1958), interacting pairs, and galaxies with high IR luminosity (ULIRG, Ultra-Luminous IR Galaxies), which resulted in revealing 1178 galaxies and 399 stars, named Byurakan-IRAS Galaxies (BIG) (Mickaelian and Sargsyan, 2004) and Byurakan-IRAS Stars (BIS) (Mickaelian and Gigoyan, 2006), respectively. Identifications using low-dispersion spectra of the First Byurakan Survey (FBS or Markarian survey) (Markarian et al., 1989) and its digitized version, DFBS (Mickaelian et al., 2007, Massaro et al., 2008) guaranteed better selection of optical counterparts compared to other identification works.

BIG objects have been studied spectroscopically using BAO 2.6 m (Mickaelian et al., 2003, Sargsyan and Mickaelian, 2006), Special Astrophysical Observatory (SAO, Russia) 6 m (Mickaelian et al., 1998, Balayan et al., 2001), Observatoire de Haute-Provence (OHP, France) 1.93 m (Mickaelian, 2004) telescopes and the Sloan Digital Sky Survey (Abolfathi et al., 2018) (Mickaelian et al., 2018). Altogether 255 BIG objects have been studied and classified. The spectroscopic studies of BIG objects facilitate the concurrent solution of several problems. These problems range from confirming the extragalactic nature of objects and determining their redshifts to detailed analyses of the objects' structure, which proved to be of greatest interest, such as galaxies with enhanced IR luminosities and/or with nuclear or starburst activity.

2. BIG Sample

A total of 257 spectra were obtained: 56 with the BAO telescope, 54 with the SAO telescope, 64 with the OHP telescope and 83 from the SDSS. The list of all objects with their parameters are given in Table 1. The columns list spectra source (telescope name or SDSS), the IRAS names for the objects, stellar magnitudes close to V (for objects from SDSS the r band was taken), the radial velocities (v_r) determined from the emission z (and calculated using the relativistic formula), the corresponding distances of the objects calculated for $H = 71\ km/(s{\times}Mpc)$, the absolute stellar magnitudes (M), the redshifts determined from the emission lines (z_{em}), and the type of activity of the objects (":" denotes objects with uncertain classifications).

Table 1: **The list of all observed BIG objects with their parameters**

IRAS source	m_V	Spectra source	z_{em}	v_r (km/s)	R (Mpc)	M	Activity type
03304+8456a	16.8	OHP 1.93m	0.0509	14868	209	-19.80	HII
03304+8456b	16.4	BAO 2.6m	0.0500	14625	206	-20.16	Abs
03333+7851	15.0	OHP 1.93m	0.0561	16347	230	-21.81	HII
03347+7748	15.5	OHP 1.93m	0.0346	10209	144	-20.29	Composite
03386+7909	15.9	OHP 1.93m	0.0559	16313	230	-20.91	Sy2
03424+8424	16.0	SAO 6m	0.0744	21492	303	-21.41	LINER:
03424+8713	15.4	BAO 2.6m	0.0249	7365	104	-19.67	HII
03485+7703	15.6	OHP 1.93m	0.0701	20281	286	-21.68	HII
04033+6942	15.9	OHP 1.93m	0.0161	4803	68	-18.25	LINER
04079+7033	14.5	OHP 1.93m	0.0132	3934	55	-19.22	HII
04140+7448	16.0	OHP 1.93m	0.0338	9972	140	-19.74	AGN
04183+7457	14.7	OHP 1.93m	0.0325	9589	135	-20.95	Composite
04574+7639	17.1	BAO 2.6m	0.1209	34081	480	-21.29	Em
05097+7954	15.2	OHP 1.93m	0.0570	16602	234	-21.64	HII

Table 1 – continued from previous page

IRAS source	m_V	Spectra source	z_{em}	v_r (km/s)	R (Mpc)	M	Activity type
05126+6516	15.4	OHP 1.93m	0.0402	11824	167	-20.71	HII
05196+7257	17.4	OHP 1.93m	0.1030	29303	413	-20.68	Sy2
05214+7741	16.3	OHP 1.93m	0.0769	22194	313	-21.17	AGN
05229+6826	14.5	OHP 1.93m	0.0166	4950	70	-19.72	HII
05275+6600	16.0	OHP 1.93m	0.0306	9037	127	-19.52	AGN:
05395+7550	15.0	OHP 1.93m	0.0248	7342	103	-20.07	HII
05401+6435	15.2	SAO 6m	0.0539	15735	222	-21.53	HII
05475+7449	16.0	OHP 1.93m	0.0515	15061	212	-20.63	Composite
05577+6141	16.1	OHP 1.93m	0.0306	9034	127	-19.42	Em
06022+7559	16.8	OHP 1.93m	0.0817	23509	331	-20.80	HII
06028+6734a	15.9	BAO 2.6m	0.0169	5015	71	-18.33	HII
06028+6734b	15.9	BAO 2.6m	0.0168	4983	70	-18.31	HII
06038+6239	14.4	SAO 6m	0.0413	12134	171	-21.76	Norm.
06261+7818a	18.4	BAO 2.6m	0.0939	26855	378	-19.45	HII
06261+7818b	17.4	BAO 2.6m	0.0940	26883	379	-20.48	LINER:
06273+6858a	17.2	BAO 2.6m	0.0664	19252	271	-19.96	Em
06273+6858b	16.4	OHP 1.93m	0.0665	19299	272	-20.77	HII
06273+6858c	15.7	OHP 1.93m	0.0656	19022	268	-21.44	Sy2
06319+7536	18.1	OHP 1.93m	0.0915	26210	369	-19.74	Composite
06432+8551	19.0	BAO 2.6m	0.0898	25743	363	-18.80	HII
06432+8551b	16.5	SAO 6m	0.0891	25544	360	-21.28	HII
06545+6647	16.1	OHP 1.93m	0.0160	4765	67	-18.03	HII
06584+6716a	17.0	BAO 2.6m	0.0734	21214	299	-20.38	Composite
06584+6716b	17.9	BAO 2.6m	0.0710	20546	289	-19.41	Unknown
07007+8242	16.9	SAO 6m	0.0586	17066	240	-20.00	HII
07021+7349	14.0	OHP 1.93m	0.1031	29335	413	-24.08	LINER:
07158+7706	15.5	OHP 1.93m	0.0485	14198	200	-21.00	HII
07205+7842	16.3	OHP 1.93m	0.0866	24859	350	-21.42	Sy2
07225+7653	16.1	OHP 1.93m	0.0484	14160	199	-20.40	AGN
07479+7832	18.3	OHP 1.93m	0.1734	47577	670	-20.83	Em
08036+7211	15.4	BAO 2.6m	0.0387	11374	160	-20.63	Em
08054+6824	14.1	OHP 1.93m	0.0413	12123	171	-22.06	Composite
08095+6445	14.1	SAO 6m	0.0294	8690	122	-21.34	Norm.
08142+6821	16.0	OHP 1.93m	0.0388	11414	161	-20.03	HII
08247+7311	14.9	OHP 1.93m	0.0655	19013	268	-22.24	HII
08259+7427	17.3	OHP 1.93m	0.1232	34685	489	-21.14	HII
08303+6118	16.8	SDSS	0.0865	24831	350	-20.89	HII
08317+7602	17.0	OHP 1.93m	0.0931	26632	375	-20.87	HII
08339+6517	14.4	BAO 2.6m	0.0190	5634	79	-20.12	HII
08379+6753	16.0	BAO 2.6m	0.0363	10687	151	-19.89	HII
08410+6124	16.3	SDSS	0.0769	22189	313	-21.18	HII
08567+6325	15.7	SDSS	0.0386	11347	160	-20.31	HII/Sy2
09002+8106	16.6	SAO 6m	0.0494	14454	204	-19.94	HII
09020+6751a	16.7	BAO 2.6m	0.0505	14754	208	-19.89	LINER
09020+6751b	16.1	BAO 2.6m	0.0564	16435	231	-20.74	Em
09037+6937	16.8	OHP 1.93m	0.0125	3738	53	-16.81	HII
09056+6538	16.3	BAO 2.6m	0.0652	18910	266	-20.88	Composite
09056+6538	16.3	SDSS	0.0649	18829	265	-20.80	HII
09062+8134a	16.8	SAO 6m	0.0495	14483	204	-19.75	LINER:
09062+8134b	17.9	SAO 6m	0.0491	14369	202	-18.63	HII
09103+8326	17.1	SAO 6m	0.0497	14540	205	-19.46	HII

Table 1 – continued from previous page

IRAS source	m_V	Spectra source	z_{em}	v_r (km/s)	R (Mpc)	M	Activity type
09162+6539	14.6	SDSS	0.0379	11143	157	-21.35	HII
09162+6539	15.5	OHP 1.93m	0.0379	11160	157	-20.48	HII
09173+6231	15.6	SDSS	0.0473	13859	195	-20.90	HII
09176+6544	15.2	SDSS	0.0190	5640	79	-19.26	HII
09180+6532	16.0	OHP 1.93m	0.0382	11230	158	-20.00	HII
09229+7731	15.0	BAO 2.6m	0.0092	2741	39	-17.93	HII
09233+7825	14.7	OHP 1.93m	0.0747	21586	304	-22.71	Em
09244+7405	17.2	OHP 1.93m	0.1586	43847	618	-21.75	Sy2
09273+6232	16.3	SDSS	0.0420	12350	174	-19.89	AGN:
09305+6813	15.7	OHP 1.93m	0.0710	20548	289	-21.61	Sy2:
09343+6450	15.8	SDSS	0.0710	20542	289	-21.53	Sy2:
09363+6655	15.9	SDSS	0.0596	17355	244	-21.04	HII
09386+6240	15.6	SDSS	0.0397	11661	164	-20.48	Em
09406+6840	15.6	SDSS	0.0118	3506	49	-17.89	HII
09406+6840	16.3	OHP 1.93m	0.0119	3561	50	-17.20	HII
09418+8124	16.0	SAO 6m	0.0398	11703	165	-20.09	Abs
09427+7528	17.6	BAO 2.6m	0.1099	31168	439	-20.61	HII
09477+7050a	18.5	SAO 6m	0.1268	35645	502	-20.00	Norm.
09477+7050b	18.0	SAO 6m	0.1270	35698	503	-20.51	HII
09477+7050c	17.5	SAO 6m	0.1277	35881	505	-21.02	HII
09571+8435	16.5	SAO 6m	0.0924	26444	372	-21.36	HII
10045+7502b	16.0	BAO 2.6m	0.0481	14083	198	-20.49	LINER
10172+7548	16.2	OHP 1.93m	0.0592	17235	243	-20.73	HII
10210+7528	15.5	OHP 1.93m	0.0279	8245	116	-19.82	HII
10228+6227	17.2	SDSS	0.1163	32871	463	-21.17	HII
10252+7013	16.0	OHP 1.93m	0.1180	33319	469	-22.36	HII
10270+7302	12.5	OHP 1.93m	0.0224	6654	94	-22.36	HII
10272+6953	14.5	OHP 1.93m	0.0387	11391	160	-21.53	Composite
10276+7443	17.3	OHP 1.93m	0.0576	16769	236	-19.57	AGN
10298+6119	15.2	SDSS	0.0293	8666	122	-20.22	HII
10331+6338	15.9	SDSS	0.0381	11202	158	-20.04	HII
10361+7952a	15.9	BAO 2.6m	0.0388	11414	161	-20.16	HII
10361+7952b	15.5	BAO 2.6m	0.0394	11587	163	-20.56	HII/Comp:
10383+7637	16.2	OHP 1.93m	0.0315	9293	131	-19.38	AGN
10486+6558	16.7	SDSS	0.0338	9960	140	-18.99	HII
10527+7136	16.4	BAO 2.6m	0.1011	28790	405	-21.68	Composite
10529+7144	14.0	OHP 1.93m	0.0619	17996	253	-23.02	HII
10541+6614	17.3	SDSS	0.1306	36641	516	-21.22	Em
10589+6515	16.1	SDSS	0.0775	22362	315	-21.40	Sy2
11008+7915a	16.7	OHP 1.93m	0.0620	18013	254	-20.32	HII
11008+7915b	16.5	OHP 1.93m	0.0620	18013	254	-20.52	HII
11053+7037	14.0	OHP 1.93m	0.0412	12097	170	-22.16	HII
11059+7117	17.9	OHP 1.93m	0.1388	38761	546	-20.79	Composite
11067+7024a	15.5	BAO 2.6m	0.0389	11443	161	-20.54	HII/Comp:
11067+7024b	16.0	BAO 2.6m	0.0389	11443	161	-20.04	HII
11069+7438	16.2	OHP 1.93m	0.0395	11602	163	-19.87	HII
11085+7712a	15.6	OHP 1.93m	0.1003	28574	402	-22.42	Composite
11085+7712b	18.0	OHP 1.93m	0.0996	28404	400	-20.01	AGN
11161+6629	15.5	SDSS	0.0431	12663	178	-20.78	HII
11201+6305	16.9	SDSS	0.1905	51799	730	-22.41	Em
11201+6305	15.7	SDSS	0.0111	3311	47	-17.66	HII

Table 1 – continued from previous page

IRAS source	m_V	Spectra source	z_{em}	v_r (km/s)	R (Mpc)	M	Activity type
11371+8106	16.7	BAO 2.6m	0.0445	13053	184	-19.60	HII
11401+6642	15.4	SDSS	0.0554	16169	228	-21.36	HII
11436+7438	14.8	OHP 1.93m	0.0560	16333	230	-22.01	Composite
11462+6424	15.3	SDSS	0.0414	12169	171	-20.87	HII
11472+6647	15.3	SDSS	0.0402	11809	166	-20.78	Sy2
11497+6139	16.0	SDSS	0.0427	12530	176	-20.21	HII
11587+6124	17.4	SDSS	0.1638	45166	636	-21.66	HII
12008+6141	15.6	SDSS	0.0644	18689	263	-21.48	HII/LINER
12040+8158	17.7	BAO 2.6m	0.0903	25858	364	-20.14	HII
12069+6753	17.1	SDSS	0.0585	17026	240	-19.83	HII
12077+8131	16.5	BAO 2.6m	0.0397	11671	164	-19.56	HII
12119+6117	17.3	SDSS	0.1630	44948	633	-21.72	Em
12120+6838	15.5	SDSS	0.0602	17512	247	-21.48	HII
12120+6838	15.5	SDSS	0.0606	17643	248	-21.44	Sy1.9
12120+6838a	15.8	BAO 2.6m	0.0581	16924	238	-21.09	HII
12120+6838b	16.2	BAO 2.6m	0.0604	17574	248	-20.77	HII
12120+6838c	15.6	BAO 2.6m	0.0597	17376	245	-21.34	Composite
12138+7537a	16.9	BAO 2.6m	0.0497	14540	205	-19.67	HII
12138+7537b	15.5	BAO 2.6m	0.0468	13712	193	-20.93	Em
12138+7537c	16.5	BAO 2.6m	0.0525	15337	216	-20.17	LINER
12147+6306	15.4	SDSS	0.0501	14656	206	-21.14	HII
12147+6306	13.9	SAO 6m	0.0505	14768	208	-22.69	Norm.
12164+6437	15.0	SDSS	0.0308	9104	128	-20.57	HII
12207+6329	15.0	SDSS	0.0589	17154	242	-21.87	HII
12226+6630	17.4	SDSS	0.0865	24819	350	-20.37	Em
12226+6630	16.4	SDSS	0.0899	25762	363	-21.45	HII
12235+6253	16.6	SDSS	0.0672	19479	274	-20.60	AGN
12267+6540	16.4	SDSS	0.0504	14728	207	-20.15	HII
12312+6939	15.4	OHP 1.93m	0.0692	20035	282	-21.85	HII
12395+6238	14.2	SAO 6m	0.0342	10085	142	-21.56	Composite
12395+6238	15.7	SDSS	0.0338	9959	140	-20.08	HII
12470+6705	17.4	SDSS	0.1295	36345	512	-21.14	HII
12477+7936a	14.7	OHP 1.93m	0.0338	9972	140	-21.04	HII
12483+7332	14.9	OHP 1.93m	0.0314	9269	131	-20.68	HII
12502+7625	16.5	OHP 1.93m	0.0634	18424	259	-20.57	HII
13014+6146	15.3	SDSS	0.0269	7968	112	-19.93	HII
13014+6146	14.0	SAO 6m	0.0272	8049	113	-21.27	Norm.
13030+6102	15.4	SAO 6m	0.0698	20211	285	-21.87	HII
13045+7016a	16.2	OHP 1.93m	0.0646	18752	264	-20.91	Em
13045+7016b	16.4	OHP 1.93m	0.0645	18736	264	-20.71	HII
13121+6646	16.0	SDSS	0.0677	19627	276	-21.20	HII
13209+6353	17.5	SDSS	0.1997	54016	761	-21.91	Sy2
13234+6239	16.0	SDSS	0.0418	12272	173	-20.17	HII
13286+7258	14.0	OHP 1.93m	0.0305	8996	127	-21.51	AGN
13291+6524	17.3	SDSS	0.0365	10738	151	-18.62	LINER:
13300+6652	17.4	SDSS	0.1044	29694	418	-20.71	AGN
13300+7219	15.2	OHP 1.93m	0.0360	10594	149	-20.67	Composite
13367+6703	17.2	SDSS	0.0933	26680	376	-20.68	HII
13386+6557	16.2	SDSS	0.0480	14047	198	-20.26	HII
13410+7837	16.0	BAO 2.6m	0.0580	16905	238	-20.93	Composite
13503+6104	16.6	SDSS	0.0880	25230	355	-21.11	HII

Table 1 – continued from previous page

IRAS source	m_V	Spectra source	z_{em}	v_r (km/s)	R (Mpc)	M	Activity type
13513+6616	15.9	SDSS	0.0702	20331	286	-21.38	HII
13524+6213	16.5	SDSS	0.0729	21076	297	-20.86	HII
13524+6213	16.8	SDSS	0.0730	21111	297	-20.53	HII
14004+7445a	15.9	BAO 2.6m	0.0670	19422	274	-21.28	HII
14004+7445b	16.5	BAO 2.6m	0.0673	19523	275	-20.67	Composite
14013+6520	16.0	SDSS	0.0345	10173	143	-19.74	HII
14129+6111	17.8	SDSS	0.1514	42024	592	-21.11	HII
14132+6552	15.4	SDSS	0.0325	9585	135	-20.22	HII
14190+6432	17.2	SDSS	0.1525	42288	596	-21.70	LINER
14196+7734	16.6	BAO 2.6m	0.0469	13732	193	-19.87	AGN
14230+6158	16.4	SDSS	0.1112	31523	444	-21.80	Sy2
14244+6435	17.8	SDSS	0.1130	31992	451	-20.49	HII/Sy1.9
14263+6116	15.7	SDSS	0.0618	17967	253	-21.28	HII
14271+6437	17.7	SDSS	0.1411	39375	555	-20.98	HII
14360+6129	14.5	SAO 6m	0.0521	15223	214	-22.16	HII
14370+6254	16.6	SDSS	0.1154	32622	459	-21.75	HII
14386+6113	16.0	SDSS	0.0934	26721	376	-21.88	HII
14418+6131A	15.0	SDSS	0.0480	14044	198	-21.53	HII/LINER
14418+6131A	15.7	SDSS	0.0492	14410	203	-20.88	HII/LINER
14418+6131A	17.5	SDSS	0.0477	13958	197	-18.93	Em
14418+6131A	17.1	SDSS	0.0494	14458	204	-19.49	HII
14436+6258	14.9	SDSS	0.0375	11036	155	-21.07	HII
14445+7003	17.0	BAO 2.6m	0.0518	15138	213	-19.65	Em
14458+7926	16.5	BAO 2.6m	0.0316	9330	131	-19.09	Sy2:/Comp
14464+6119	16.9	SDSS	0.1364	38151	537	-21.76	Sy1.2
14501+6212	14.9	SAO 6m	0.0429	12594	177	-21.34	Abs
14501+6212	15.0	SDSS	0.0431	12666	178	-21.23	HII
14561+6312	14.7	SAO 6m	0.0432	12680	179	-21.56	Norm.
14561+6312	15.2	SDSS	0.0426	12510	176	-21.08	Sy2
14570+6339	16.2	SAO 6m	0.0475	13912	196	-20.26	LINER
14574+7641a	16.5	BAO 2.6m	0.0446	13082	184	-19.83	HII
15356+6119a	16.4	SAO 6m	0.0886	25407	358	-21.37	HII
15356+6119b	14.4	SAO 6m	0.0882	25297	356	-23.36	HII
15374+6822	15.7	BAO 2.6m	0.0578	16851	237	-21.17	HII
15427+6141	17.6	SAO 6m	0.0573	16698	235	-19.26	Norm.
15449+6459	15.3	SAO 6m	0.0373	10981	155	-20.65	Norm.
16030+6312a	16.8	SAO 6m	0.0548	15990	225	-19.96	Norm.
16030+6312b	15.9	SAO 6m	0.0569	16585	234	-20.94	HII
16044+6727	16.1	BAO 2.6m	0.0233	6906	97	-18.85	HII
16049+8802	16.8	BAO 2.6m	0.0541	15803	223	-19.95	Sy2
16101+6345	16.5	SAO 6m	0.0563	16415	231	-20.32	HII
16118+6231	13.3	SAO 6m	0.0321	9476	133	-22.33	Composite
16119+8551	17.1	BAO 2.6m	0.0847	24335	343	-20.54	HII
16358+6709a	15.0	BAO 2.6m	0.0534	15593	220	-21.69	Em
16358+6709b	15.0	BAO 2.6m	0.0537	15687	221	-21.70	HII
16365+6403a	15.7	SAO 6m	0.0628	18250	257	-21.35	HII
16365+6403b	17.5	SAO 6m	0.0628	18250	257	-19.55	HII
16365+6403c	12.6	SAO 6m	0.0632	18362	259	-24.46	HII
16452+6418a	16.3	SAO 6m	0.0697	20183	284	-20.97	Sy2
16452+6418b	16.6	SAO 6m	0.0684	19820	279	-20.63	HII
16452+6418c	14.2	SAO 6m	0.0685	19848	280	-23.03	HII

Table 1 – continued from previous page

IRAS source	m_V	Spectra source	z_{em}	v_r (km/s)	R (Mpc)	M	Activity type
16452+6418d	17.1	SAO 6m	0.0697	20183	284	-20.17	HII
16533+6216	16.1	SDSS	0.1059	30089	424	-22.03	HII
16588+6357	15.6	SDSS	0.0604	17568	247	-21.40	Em
17008+6444	15.0	SDSS	0.0273	8076	114	-20.26	HII
17008+6444	12.6	SAO 6m	0.0278	8224	116	-22.72	HII
17017+6416	15.2	SDSS	0.0843	24238	341	-22.43	HII
17017+6416	14.1	SAO 6m	0.0848	24365	343	-23.58	HII
17037+6207	17.2	SDSS	0.1558	43138	608	-21.73	Em
17037+6207	15.8	SDSS	0.0823	23669	333	-21.86	HII
17046+6255	16.4	SDSS	0.0883	25318	357	-21.39	HII
17046+6255	20.6	SDSS	0.0874	25086	353	-17.17	HII
17062+7544	16.1	BAO 2.6m	0.0654	18974	267	-21.02	Em
17089+6558	17.3	SDSS	0.0278	8238	116	-18.04	HII/LINER
17089+6558a	17.6	BAO 2.6m	0.0279	8256	116	-17.73	HII
17089+6558b	15.6	BAO 2.6m	0.0282	8335	117	-19.75	HII
17102+6442	16.1	SDSS	0.0789	22735	320	-21.42	HII
17102+6442	14.4	SAO 6m	0.0789	22739	320	-23.13	HII
17173+6119	15.7	SDSS	0.0717	20732	292	-21.67	HII
17173+6119	14.7	SAO 6m	0.0735	21242	299	-22.68	Composite
17190+6219	16.7	SDSS	0.0803	23117	326	-20.84	AGN
17190+6219	17.0	SAO 6m	0.0808	23264	328	-20.58	Norm.
17207+6307	15.4	SDSS	0.0338	9972	140	-20.30	HII
17207+6307	15.3	SAO 6m	0.0336	9911	140	-20.42	HII
17330+7619	17.2	BAO 2.6m	0.0769	22185	312	-20.26	HII
17349+6139a	16.2	SAO 6m	0.0858	24639	347	-21.50	HII
17349+6139b	18.8	SAO 6m	0.0862	24749	349	-18.91	Norm.
17442+6130	14.0	SAO 6m	0.0365	10750	151	-21.90	Norm.
17469+6416	14.6	SAO 6m	0.0355	10461	147	-21.24	HII
17552+6209	16.4	SAO 6m	0.0836	24035	339	-21.25	Sy2
17591+8628	15.2	BAO 2.6m	0.0233	6917	97	-19.72	HII
18116+6328	13.9	SAO 6m	0.0481	14083	198	-22.59	Norm.
18169+6433c	12.4	SAO 6m	0.0208	6175	87	-22.30	HII
18169+6433d	15.1	SAO 6m	0.0209	6204	87	-19.61	HII
18192+8650	16.3	BAO 2.6m	0.0655	19002	268	-20.88	HII
18247+6102	15.7	SAO 6m	0.0732	21158	298	-21.67	LINER
18252+6315	15.9	SAO 6m	0.0838	24090	339	-21.75	HII
18380+8640b	16.1	BAO 2.6m	0.0778	22435	316	-21.43	HII
18380+8640c	16.0	BAO 2.6m	0.0779	22451	316	-21.46	HII
20537+8737	14.8	BAO 2.6m	0.0195	5784	81	-19.77	Em

The objects have redshifts in the range $0.0092 < z < 0.1997$ and absolute stellar magnitudes in the range -16.81 $< M <$ -24.46. The distribution of redshifts is given in Fig. 1 and the distribution of absolute magnitudes is given in Fig. 2.

3. Summary and conclusion

Spectral observations of BIG objects at the BAO 2.6-m, SAO 6-m, OHP 1.93-m telescopes and taken from SDSS database have yielded a fairly rich set of data for studying IR galaxies. These data can be used to study the BIG sample, and also to compare these objects with IR galaxies from other samples. A total of 257 BIG objects were observed; of these 149 were identified as galaxies with star formation regions, 42 as AGN, 28 as galaxies with a composite spectrum (referred below

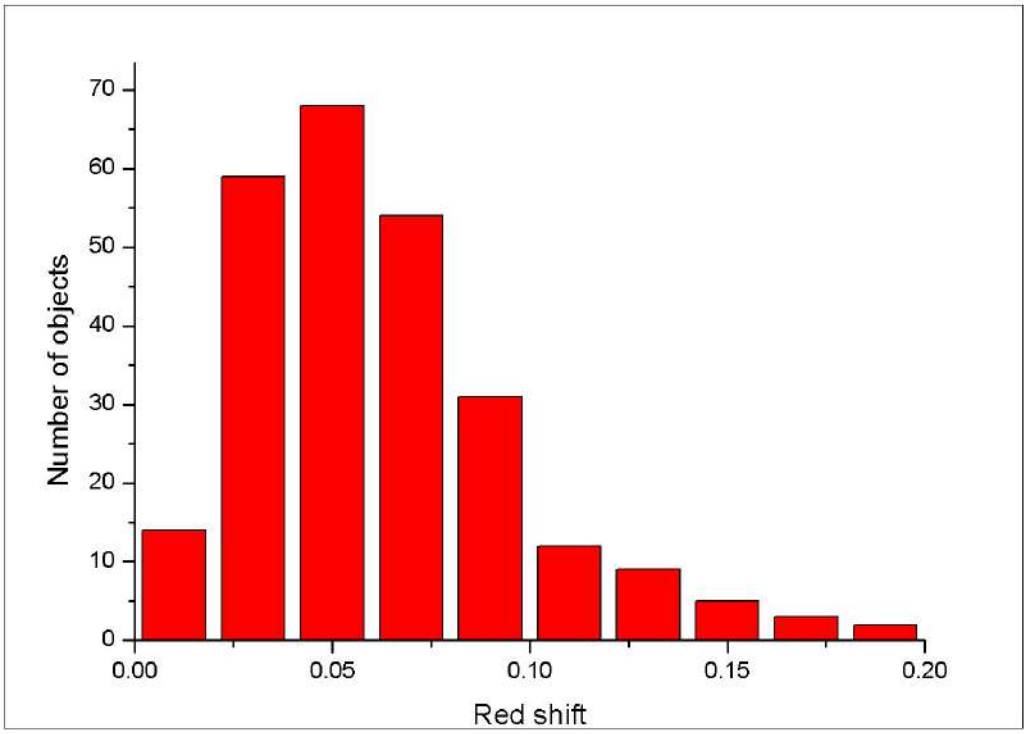

Figure 1. Distribution of redshifts

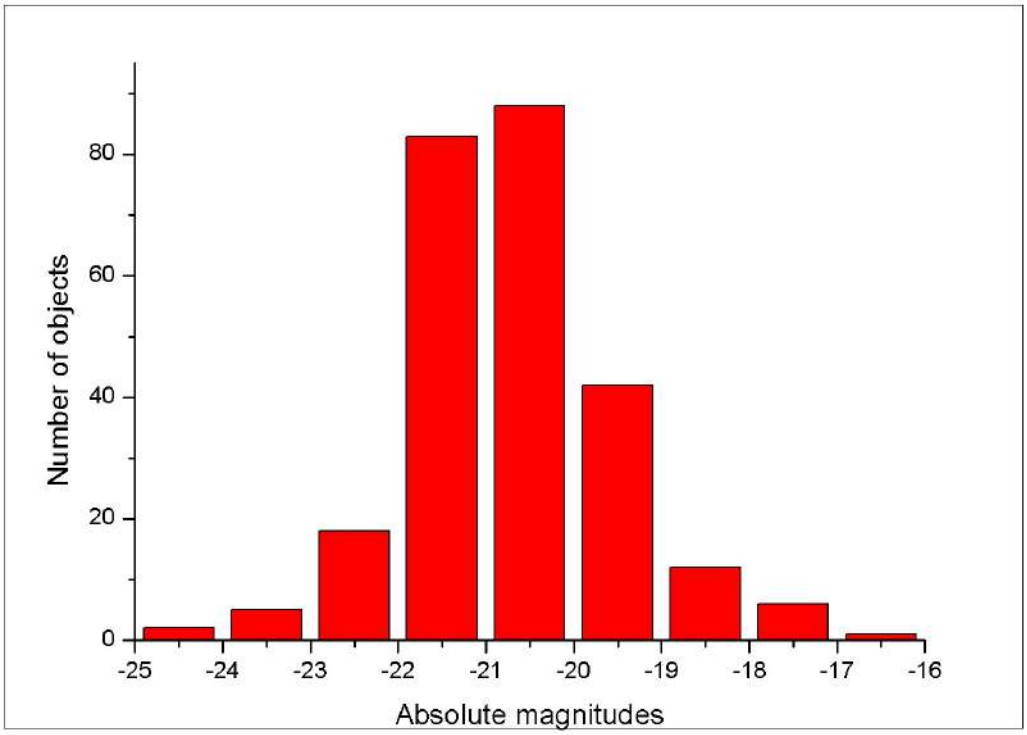

Figure 2. Distribution of absolute magnitudes

to Composite or Comp), 21 as "Em" galaxies (this type refers to a spectrum with signs of emission without the possibility of a more precise determination of the activity class of the galaxy), 13 as galaxies represented as Norm (galaxies for which the rate of star formation does not exceed the normal), 3 as

absorption galaxy and one object without the possibility of classification (unknown). In Table 2 the distribution of all objects by activity types is given.In Fig. 3 absolute magnitude (M) vs redshift (z) is given.

Table 2: The distribution of 257 BIG objects by activity types

Activity type	**Number of objects**	%	**Activity type**	**Number of objects**	%
HII	149	58.0	AGN	13	5.1
Composite	22	8.6	Em	21	8.2
HII / LINER	4	1.5	Norm	13	5.1
HII / Sy	2	0.8	Abs	3	1.1
LINER	12	4.6	Unknown	1	0.4
Sy	17	6.6	**All**	**257**	**100.0**

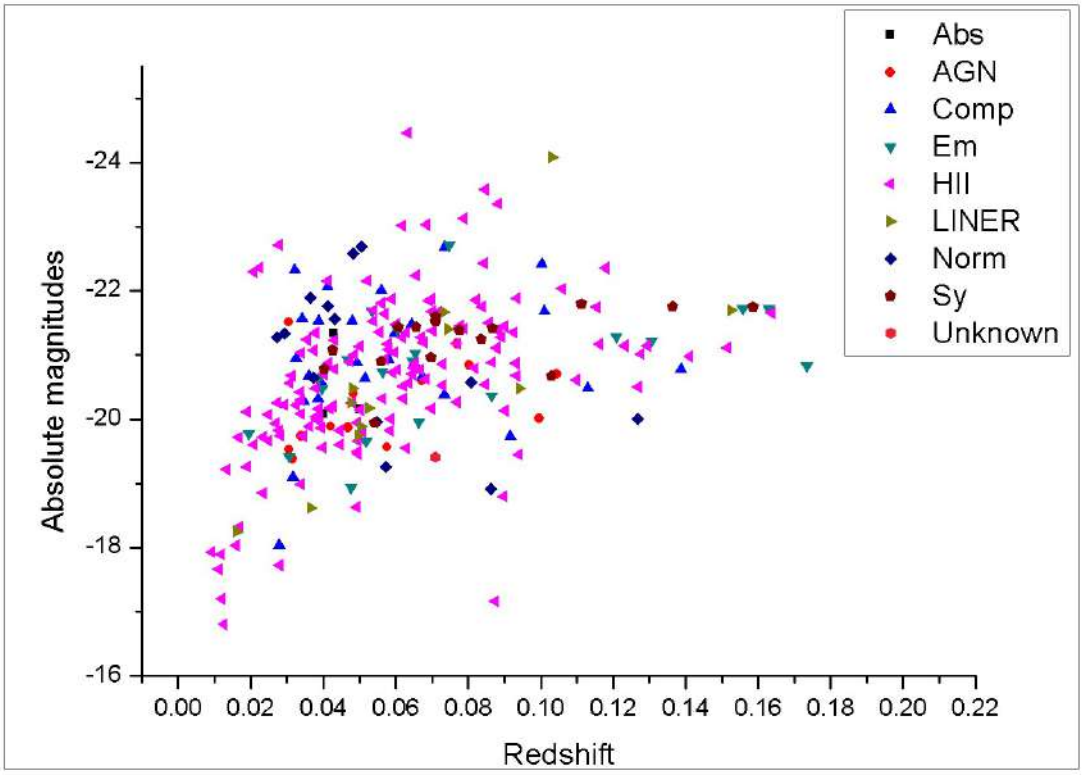

Figure 3. The distribution of absolute magnitudes vs redshifts

Besides isolated galaxies, the observed objects include some binary and multiple systems. This makes it possible to establish their physical coupling, to determine the true IR source more precisely (as an individual galaxy or the system as a whole), and to study the interrelation between star formation activity, the interactions of galaxies, and the activity of their nuclei.

References

M. Moshir, G. Kopan, T. Conrow, and et al. *Infrared Astronomical Satellite Catalogs, The Faint Source Catalog, Version 2.0*, 1990.

H.V. Abrahamyan, A.M. Mickaelian, and A.V. Knyazyan. *Astron. Comput. 10, 99*, 2015.

D.B. Sanders and I.F. Mirabel. *Luminous Infrared Galaxies, Ann. Rev. Astron. Astrophys. 34, 749*, 1996.

R.M. Cutri, M.F. Skrutskie, S. van Dyk, and et al. *2MASS All-Sky Catalog, Univ. Mass. and IPAC/CalTech*, 2003.

M.F. Skrutskie, R.M. Cutri, R. Stiening, M.D. Weinberg, S. Schneider, J.M. Carpenter, C. Beichman, R. Capps, and et al. *Astron. J. 131, 1163*, 2006.

R.M. Cutri, E.L. Wright, T. Conrow, and et al. *WISE All-Sky DR, IPAC/Caltech*, 2013.

D. Ishihara, T. Onaka, H. Kataza, A. Salama, C. Alfageme, A. Cassatella, N. Cox, P.García-Lario, and et al. *Astron. Astrophys. 514, 1*, 2010.

I. Yamamura, S. Makiuti, N. Ikeda, Y. Fukuda, S. Oyabu, T. Koga, and G.J. White. *AKARI/FIS, ISAS/JAXA*, 2010.

D.B. Sanders, J.M. Mazzarella, D.-C. Kim, J.A. Surace, and B. T. Soifer. *Astron. J. 126, 1607*, 2003.

E. Bertin, M. Dennefeld, and M. Moshir. *Astron. Astrophys. 323, 685*, 1997.

M.A. Strauss and J.P. Huchra. *Astron. J. 95, 1602*, 1988.

G. Wang, S.K. Leggett, R.G. Clowes, H.T. MacGillivray, and A. Savage. *MNRAS 248, 112*, 1991.

K.B. Fisher, J.P. Huchra, M.A. Strauss, M. Davis, A. Yahil, and D. Schlegel. *Astrophys. J. Suppl. Ser. 100, 69*, 1995.

Q.R. Yuan, Z.H. Zhu, Z.L. Yang, and X.T. He. *Astron. Astrophys. Suppl. Ser. 115, 267*, 1996.

A.M. Mickaelian. *Astrophysics 38, 625*, 1995.

D.W. Weedman, F.R. Feldman, V.A. Balzano, and et al. *Astrophys. J. 248, 105*, 1981.

V.A. Ambartsumian. *XI Solvay Conference, Editions Stoops, Brussels*, 1958.

A.M. Mickaelian and L.A. Sargsyan. *Astrofizika 47, 109*, 2004.

A.M. Mickaelian and K.S. Gigoyan. *Astron. Astrophys. 455, 765. Catalog No. III/237a in Vizier, CDS, Strasbourg*, 2006.

B.E. Markarian, V.A. Lipovetsky, J.A. Stepanian, L.K. Erastova, and A.I. Shapovalova. *Comm. SAO 62, 5*, 1989.

A.M. Mickaelian, R. Nesci, C. Rossi, D. Weedman, G. Cirimele, L.A. Sargsyan, L.K. Erastova, K.S. Gigoyan, and et al. *Astron. Astrophys. 464, 1177*, 2007.

E. Massaro, A.M. Mickaelian, R. Nesci, and D. Weedman. *The Digitized First Byurakan Survey (Roma, Italy)*, 2008.

A.M. Mickaelian, L.R. Oganesyan, and L.A. Sargsyan. *Astrofizika 46, 221*, 2003.

L.A. Sargsyan and A.M. Mickaelian. *Astrofizika 49, 19*, 2006.

A.M. Mickaelian, S.A. Akopyan, S.K. Balayan, and A.N. Burenkov. *Pis'ma v Astron. zh. 24, 736*, 1998.

S.K. Balayan, S.A. Akopyan, A.M. Mickaelian, and A.N. Burenkov. *Pis'ma v Astron. zh. 27, 330*, 2001.

A.M. Mickaelian. *Astrofizika 47, 425*, 2004.

B. Abolfathi, D.S. Aguado, G. Aguilar, and et al. *The Astrophysical Journal Supplement Series, 235, issue 2, article id. 42, p. 19*, 2018.

A.M. Mickaelian, G.S. Harutyunyan, and A. Sarkissian. *Astronomy Letters, Volume 44, Issue 6, pp.351-361*, 2018.

Joint IRAS Science Working Group. *Infrared Astronomical Satellite Catalogs, The Point Source Catalog, Version 2.0, NASA RP-1190*, 1988.